Vol. 515: 33–44, 2014
doi: 10.3354/meps10999

MARINE ECOLOGY PROGRESS SERIES
Mar Ecol Prog Ser

Published November 18

Reefs shift from net accretion to net erosion along a natural environmental gradient

Nyssa J. Silbiger[1,*], Òscar Guadayol[1,2], Florence I. M. Thomas[1], Megan J. Donahue[1]

[1]University of Hawai'i at Mānoa, Hawai'i Institute of Marine Biology, PO Box 1346, Kāne'ohe, Hawai'i 96744, USA

[2]*Present address:* University of Lincoln, School of Life Sciences, Joseph Banks Laboratories, Green Lane, Lincoln LN6 7DL, UK

ABSTRACT: Coral reefs persist in an accretion-erosion balance and ocean acidification resulting from anthropogenic CO_2 emissions threatens to shift this balance in favor of net reef erosion. Corals and calcifying algae, largely responsible for reef accretion, are vulnerable to environmental changes associated with ocean acidification, but the direct effects of lower pH on reef erosion has received less attention, particularly in the context of known drivers of bioerosion and natural variability. This study examines the balance between reef accretion and erosion along a well-characterized natural environmental gradient in Kāne'ohe Bay, Hawai'i using experimental blocks of coral skeleton. Comparing before and after micro-computed tomography (µCT) scans to quantify net accretion and erosion, we show that, at the small spatial scale of this study (tens of meters), pH was a better predictor of the accretion-erosion balance than environmental drivers suggested by prior studies, including resource availability, temperature, distance from shore, or depth. In addition, this study highlights the fine-scale variation of pH in coastal systems and the importance of microhabitat variation for reef accretion and erosion processes. We demonstrate significant changes in both the mean and variance of pH on the order of meters, providing a local perspective on global increases in pCO_2. Our findings suggest that increases in reef erosion, combined with expected decreases in calcification, will accelerate the shift of coral reefs to an erosion-dominated system in a high-CO_2 world. This shift will make reefs increasingly susceptible to storm damage and sea-level rise, threatening the maintenance of the ecosystem services that coral reefs provide.

KEY WORDS: Coral reefs · pH · Bioerosion · Accretion-erosion balance · Environmental variability · Ocean acidification

INTRODUCTION

Ocean acidification is threatening the persistence of coral reef ecosystems (Hoegh-Guldberg et al. 2007). The oceans have absorbed ~30% of the anthropogenic increase in carbon dioxide (CO_2), resulting in a decrease in the pH of ocean water ('ocean acidification') and a shift in the chemical equilibrium towards dissolution (Caldeira & Wickett 2003, Feely et al. 2004, Sabine et al. 2004). Current IPCC models predict changes in pH for the open ocean, but these mean predictions are problematic for coral reefs, which are embedded in highly variable coastal ecosystems (Gagliano et al. 2010, Hofmann et al. 2011) where restricted water motion, terrestrial influences, and feedbacks between benthic productivity and calcification strongly influence the physicochemical environment (Yates et al. 2007, Drupp et al. 2011, Massaro et al. 2012, Duarte et al. 2013, Smith et al. 2013). In this variable coastal environment, coral reef organisms experience biologically-relevant daily variation in pH (Price et al. 2012) and the magnitude of this variation changes over small spatial scales (meters to tens of meters) that are relevant to individ-

*Corresponding author: silbiger@hawaii.edu

ual organisms (Guadayol et al. 2014). This natural spatial and temporal variation can exceed the 0.07 to 0.33 pH unit increase predicted for the global oceans in the 21st century (Bopp et al. 2013), demonstrating the need to study reef processes on finer spatial and temporal scales than prior studies and presenting an opportunity to examine ecological responses to environmental variation *in situ*. Here, we take advantage of the high spatial variability in lagoon reef systems and directly measure net reef accretion and erosion in experimental blocks of coral skeleton along a natural environmental gradient.

Coral reef ecosystems persist in a balance between accretion and erosion; this balance is vulnerable to observed and predicted changes in ocean carbonate chemistry. While the response of calcifying organisms to ocean acidification is variable (Ries et al. 2009), calcification rates for most tropical coral species and other reef calcifiers decline with increasing pCO_2 (Kroeker et al. 2010, Pandolfi et al. 2011). However, these demonstrated declines may underestimate the impact of ocean acidification because net reef accretion, or growth, depends not only on the constructive process of reef calcification, but also the destructive processes of reef dissolution and bioerosion, i.e. the removal of lithic substrate by bioeroding organisms (Neumann 1966). For reefs to persist, reef accretion must exceed erosion. Reef erosion by a diverse community of grazers (fish and urchins) and internal eroders (sponges, marine worms, bivalves, and microboring flora) plays a major role in the calcium carbonate ($CaCO_3$) budget (reviewed in Hutchings 1986). Reef eroders are responsible for 90% of coral reef sediment production and just over half of these sediments are re-incorporated back into the coral framework (Hubbard et al. 1990). In addition, bioerosion increases the porosity of the coral reef framework, which provides shelter for cryptic organisms (Moran & Reaka 1988) but also reduces mechanical stability (Scott & Risk 1988).

Reef bioerosion rates respond strongly to eutrophication (e.g. Rose & Risk 1985, Edinger et al. 2000, Holmes 2000, Holmes et al. 2000, Le Grand & Fabricius 2011) and substrate type (Highsmith 1981, Risk et al. 1995, Edinger & Risk 1996, Perry 1998, Schönberg 2002). Distance from shore (Risk et al. 1995, Tribollet et al. 2002) and depth (Perry 1998, Le Grand & Fabricius 2011, Schmidt & Richter 2013) are also common correlates of bioerosion rates. However, the *in situ* response of erosion rates to pH and temperature — the variables most relevant to climate change — remains poorly characterized. Recent reviews suggest that reef erosion will increase in a high CO_2 world (Hoegh-Guldberg et al. 2007, Guinotte & Fabry 2008, Andersson & Gledhill 2013) and that reefs may shift from an accretion-dominated to an erosion-dominated state (Silverman et al. 2009), making them more susceptible to storm damage and sea-level rise (Hutchings 1986). Yet, there is little field data testing a pH-driven shift from accretion to erosion *in situ*. Laboratory studies of bioerosion response to ocean acidification have focused on specific bioeroding groups and shown increases in the penetration depth and erosion rates of microboring flora (Tribollet et al. 2009, Reyes-Nivia et al. 2013) and the boring sponge, *Cliona orientalis* (Wisshak et al. 2012, 2013, Fang et al. 2013), under elevated pCO_2 conditions. Field studies have been indirect or strongly confounded by other environmental variables: Fabricius et al. (2011) showed that the density of externally visible borer orifices in live *Porites* sp. were higher in closer proximity to CO_2 seeps in Papua New Guinea (Fabricius et al. 2011). Manzello et al. (2008) compared 3 sites in the eastern tropical Pacific and found that erosion rates were higher at sites with frequent upwelling of water with a low aragonite saturation state (Manzello et al. 2008), but these upwelling sites also had high nutrients and low temperature: temperature and nutrients are both known drivers of bioerosion (Le Grand & Fabricius 2011, Davidson et al. 2013).

In this study, we took advantage of the natural pH variation in coral reef ecosystems emphasized by recent studies (Gagliano et al. 2010, Hofmann et al. 2011, Guadayol et al. 2014) and directly measured net reef accretion and erosion using experimental blocks of coral skeleton in response to natural pH variation. This experimental approach integrated a natural, early successional community of bioeroders (including internal eroders and external grazers) and reef calcifiers, but excluded accretion by corals. To calculate net reef accretion and erosion, we used micro-computed tomography (µCT) to create high resolution (100 µm), 3-dimensional (3D) density profiles of experimental $CaCO_3$ blocks before and after deployment (see Fig. 2 below). Previous studies have used µCT to visualize bioerosion by sponges (Schönberg & Shields 2008) and to examine coral skeletal morphology (Roche et al. 2011); we applied this technology in a novel way to quantify net accretion and erosion more precisely than buoyant weight methods. Using a model-comparison framework, we compared pH with other known drivers and correlates of the accretion-erosion balance, including resource availability for filter feeding bioeroders, temperature, depth, and distance from shore.

MATERIALS AND METHODS

Study site and experimental design

Study site. The study site is located in Kāne'ohe Bay, O'ahu on the windward (eastern) side of Moku o Lo'e (Coconut Island), adjacent to the Hawai'i Institute of Marine Biology (21° 25.98' N, 157° 47.18' N) (Fig. S1 in Supplement 1 at www.int-res.com/articles/suppl/m515p033_supp/). This fringing reef is dominated by *Porites compressa* and *Montipora capitata*, with occasional colonies of *Pocillopora damicornis, Fungia scutaria,* and *Porites lobata*. Kāne'ohe Bay is a protected, semi-enclosed embayment; the residence time can be >1 mo in the protected southern portion of Kāne'ohe Bay, where our study was located (Lowe et al. 2009a). Wave action is low (Smith et al. 1981, Lowe et al. 2009b,a), and currents are moderate (5 cm s^{-1} maximum) and tidally driven (mean and maximum tidal ranges are 0.7 and 1.1 m, respectively) (Lowe et al. 2009a,b). Daily averages in pH, temperature, and O_2 in the Kāne'ohe Bay waters just offshore our site ranged from 7.83 to 8.03, 21.84 to 27.86°C, and 5.82 to 7.81 mg l^{-1}, respectively, during our study period (Guadayol et al. 2014; data for the entire transect is presented in Table S1 in Supplement 1).

Experimental design. Twenty-one experimental blocks were deployed along a 32 m transect perpendicular to the shore, stratified between reef flat and reef slope (Fig. 1e). Blocks were cable-tied to D-rings that were epoxied to the substrate and deployed from March 31, 2011 to April 10, 2012 (Fig. S2 in Supplement 1). Water samples for nutrients, chlorophyll *a*, total alkalinity (TA), and pH_T (i.e. pH on the total scale, hereafter 'pH') were collected directly above each block 4 times within 24 h in September, December, and April in order to capture both diel and seasonal variability in the environment. In addition to discrete water samples, we measured high frequency (0.1 min^{-1}) variation in temperature and depth using a continuous sensor stationed over each block for a minimum of 2 wk. These short time series were nor-

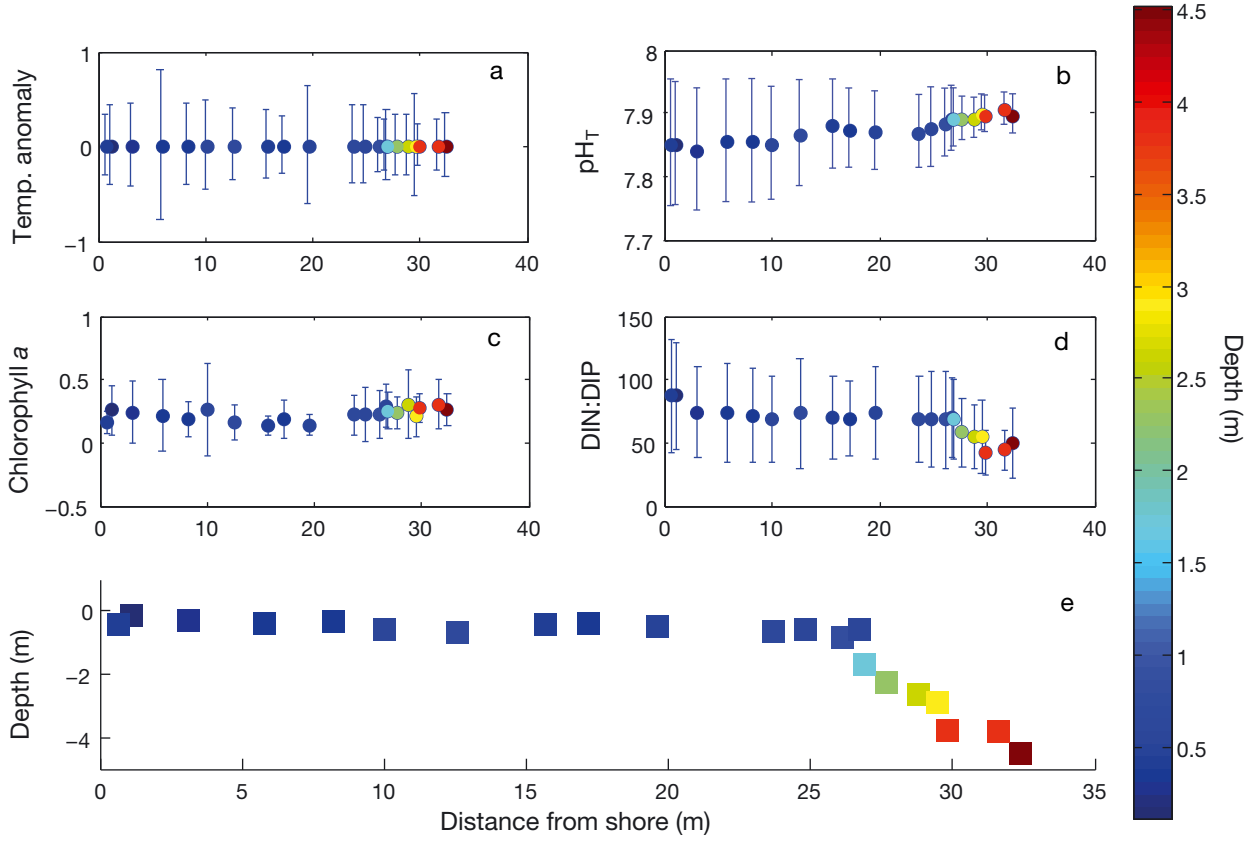

Fig. 1. Environmental parameters measured at 21 points along a coral reef transect in Kāne'ohe Bay, Hawai'i, where experimental blocks of dead coral were sampled to compare pH with other known drivers and correlates of the accretion-erosion balance: (a) relative temperature anomalies; (b) pH (total scale); (c) chlorophyll *a* (µg l^{-1}); (d) DIN:DIP; (e) the depth and distance from shore of each experimental block. In panels (a) to (d), circles and error bars show means and standard deviations of the variable at each point along the transect. The *x*-axes indicate position (m) on the the transect with 0 being closest to shore, and colors represent depth (m) as shown in the color bar

malized to a continuous time series from a permanent station positioned adjacent to the transect, allowing comparison of the micro-environments at each block (Guadayol et al. 2014). Spatial variation in the mean and variance of environmental parameters across the transect allowed comparison of potential drivers of the accretion-erosion balance (Fig. 1, Figs. S3 & S4 in Supplement 1, Table 1).

Experimental blocks. Blocks were cut from dead pieces of massive *Porites* sp. skeleton collected above the high-tide mark from beaches around O'ahu (Fig. S2). Only coral pieces with obvious calices and no visible external borings were selected. Coral pieces were cut into 5 × 5 × 2 cm blocks, soaked in fresh water, and then autoclaved to remove any living organisms. Because substrate skeletal density can influence reef bioerosion rates (Highsmith 1981, Schönberg 2002), we used blocks with similar skeletal densities. The average (±SD) skeletal density of each coral block was 1.57 ± 0.07 g cm^{-3}. The skeletal density of *Porites lobata* ranges from 1.27 to 1.66 g cm^{-3} on O'ahu and from 1.15 to 1.95 g cm^{-3} across the Hawaiian Archipelago (Grigg 1982).

Micro-computed tomography (µCT). Net accretion and erosion rates were calculated using µCT, an X-ray technology that non-destructively images the external and internal structures of solid objects, resulting in a 3D array of object densities (Fig. 2). Previous studies have used single CT scans to analyze bioerosion (Becker & Reaka-Kudla 1996, Beuck et al. 2007, Schönberg & Shields 2008, Crook et al. 2013). We used µCT in a novel way by comparing pre- and post-deployment scans. This technique allowed us to calculate a very accurate rate for net accretion-erosion and to account for and digitally remove the effect of any pre-existing borings in the experimental substrate. Further, we were able to visualize new erosion scars by external and internal eroders and new growth by secondary calcifiers in 3 dimensions, information that cannot be acquired

Table 1. Model selection for comparison of pH with other known drivers and correlates of the accretion-erosion balance on 21 experimental blocks of dead coral sampled along a transect in Kāne'ohe Bay, Hawai'i. k: number of parameters in the model; $-\log(\mathcal{L})$: negative log likelihood of the model; AIC_c: the corrected Aikaike Information Criterion; ΔAIC_c: difference from the lowest AIC_c value; R^2: proportion of total variance explained by the model; Rank: rank of the model, with 1 being the best fit. See Table S5 in Supplement 1 at www.int-res.com/articles/suppl/m515p033_supp/ for a list of environmental parameters considered and their ranges. Each model is a linear regression of net reef erosion versus the means ($\bar{X}$) and variances (Var(X)) or covariances (Covar) of each parameter. The Resource Availability Model includes the ratio of dissolved inorganic nitrogen to dissolved inorganic phosphate (DIN:DIP) and chlorophyll *a* concentration. The Full Model includes means and variances for all listed environmental parameters. The upper table (a) shows a model comparison for all measured environmental parameters (which include both means and variances of each parameter) and the lower table (b) shows the model selection for only pH mean versus variance

Model parameters	k	$-\log(\mathcal{L})$	AIC_c	ΔAIC_c	R^2	Rank
(a) Model selection comparing pH and other environmental parameters						
pH $Y \sim \overline{pH} + \mathrm{Var}(pH)$	4	−30.46	68.42	0.00	0.64	1
Depth $Y \sim \overline{Depth}$	3	−40.01	84.73	16.30	0.06	2
Distance $Y \sim Distance$	3	−40.40	85.50	17.08	0.02	3
Temperature $Y \sim \overline{Temp} + \mathrm{Covar}(Temp)$	4	−40.42	88.33	19.91	0.03	4
Resource availability $Y \sim \overline{Chl} + \mathrm{Var}(Chl) + \overline{N{:}P} + \mathrm{Var}(N{:}P)$	6	−38.91	92.11	23.68	0.18	5
Full model $Y \sim \overline{pH} + \mathrm{Var}(pH) + \overline{Temp} + \mathrm{Covar}(Temp) + \overline{Chl} + \mathrm{Var}(Chl) + \overline{N{:}P} + \mathrm{Var}(\overline{N{:}P}) + \overline{Depth} + Distance$	12	−25.92	106.84	38.42	0.82	6
(b) Model selection considering only pH mean and variance						
pH mean $Y \sim \overline{pH}$	3	−30.41	65.52	0.00	0.64	1
pH mean and variance $Y \sim \overline{pH} + \mathrm{Var}(pH)$	4	−30.46	68.42	2.90	0.64	2
pH variance $Y \sim \mathrm{Var}(pH)$	3	−39.34	83.39	17.87	0.12	3

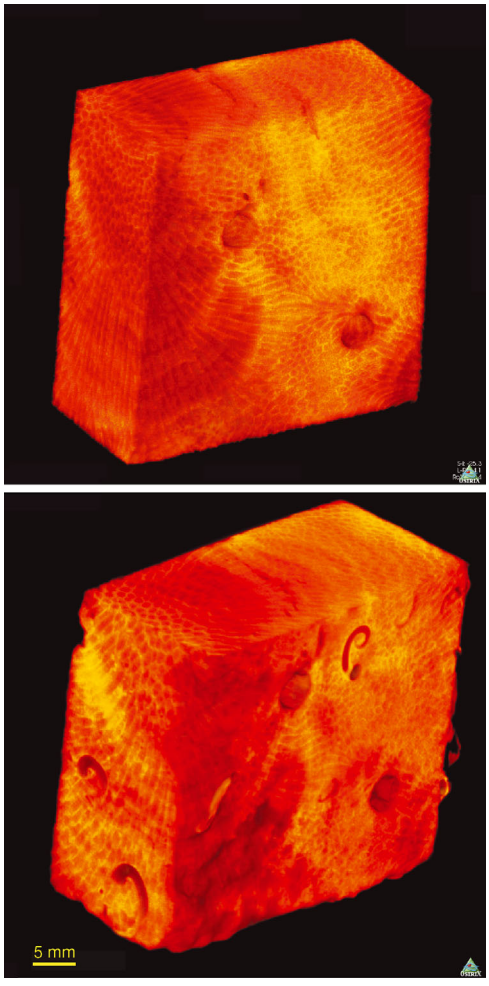

Fig. 2. Visualization of micro-computed tomography (µCT) scan of an experimental block of coral before (top) and after 1 yr deployment (bottom). See movie of the full 3D visualization of the µCT images in Supplement 2 at www.int-res.com/articles/suppl/m515p033_supp/

from traditional buoyant weight techniques. We used an eXplore CT120 µCT (GE Healthcare Xradia) at the Cornell University Imaging Multiscale CT Facility to scan blocks before and after deployment (voltage = 100 kV, current = 50 mA). Angular projections were acquired in a full 360° rotation in 0.5° increments; 2 images at each angle were acquired and averaged. A 3D array of isotropic voxels at 50 µm resolution was generated using the GE Console Software. These 50 µm voxels were averaged to 100 µm for data analysis. The intensity value in each voxel is directly related to the density of the object at that voxel. A global threshold value of 200 Hounsfield Units (HU) was used to separate $CaCO_3$ from air and remove any effects of partial volume averaging at the coral block-air interface (Roche et al. 2010). The number of voxels exceeding this threshold was multiplied by the voxel size $(100\ \mu m)^3$ to give the total volume of $CaCO_3$. We measured net accretion-erosion as the change in volume of $CaCO_3$ from before and after scans. Note that this volumetric analysis measures changes at the voxel scale of 50 µm, which was then averaged to 100 µm, and may, therefore, underestimate erosion by microborers, which make erosion scars between 1 and 100 µm (Tribollet 2008). The values were square-root transformed to meet model assumptions of normality, and 1 block with a large aggregation of oysters was excluded from the analysis.

Environmental parameters: potential predictors and correlates of net reef erosion

Sampling technique. Previous studies have identified nutrient concentration (e.g. Rose & Risk 1985, Edinger et al. 2000, Holmes 2000, Holmes et al. 2000, Le Grand & Fabricius 2011), chlorophyll (Le Grand & Fabricius 2011), temperature (Davidson et al. 2013), pH (Tribollet et al. 2009, Wisshak et al. 2012, 2013, Reyes-Nivia et al. 2013, Fang et al. 2013) and depth (Perry 1998, Le Grand & Fabricius 2011, Schmidt & Richter 2013) as possible drivers of the accretion-erosion balance. This study compared the effect of these environmental parameters on net accretion-erosion using data obtained from discrete water samples (pH, TA, nitrate (NO_3^-), nitrite (NO_2^-), ammonium (NH_4^+), phosphate (PO_4^{3-}), and chlorophyll *a*) and from continuous sensors (temperature and depth) along the transect. The discrete water samples were collected directly above each block within 2 d of spring tide at 08:00, 14:00, 20:00 h, and 02:00 h on September 10–11, 2011, December 12–13, 2011, and April 4–5, 2012. All discrete water samples were collected using snorkel or SCUBA using 60 and 120 ml plastic syringes. Syringes and storage vials were all pre-cleaned in a 10% HCl bath for 24 h and rinsed 3 times with MilliQ water; during sample collection and processing they were rinsed 3 times with sample water. The environment was sampled more continuously for temperature and depth (sampling rate of ~0.1 min^{-1}) using 1 permanent and 2 mobile monitoring stations. Two mobile stations were deployed at a time, one on the reef flat and one on the reef slope, to get simultaneous measurements at 2 different blocks on the transect. Mobile stations (Sonde 600XLM, YSI) were positioned 5 to 10 cm above each block for a 2-wk period between May 2011 and March 2012. Blocks were sampled in ran-

dom order, ensuring that the spatial gradient along the transect was not systematically confounded by temporal trends or seasonality (Guadayol et al. 2014). The permanent monitoring station (Sonde 6600-V2-4, YSI) was mounted on a pole a few meters away from the transect, downward facing at 1.7 m depth over a 3 m deep bottom, with sensors for temperature, depth, conductivity, pH, and O_2 to characterize the background water column conditions for the duration of the experiment. All multi-parametric probes were calibrated periodically using standard procedures and calibration solutions. The permanent station was recovered, cleaned, calibrated, and re-deployed 3 times during the study, and the mobile station probes were calibrated 7 times. Pre-calibration measurements of commercial standard solutions were conducted to detect sensor drift, although none was found for the period of study. The background water column data are reported in Guadayol et al. (2014).

Nutrients and chlorophyll. Water samples collected for nutrients were immediately filtered through combusted 25mm glass fiber filters (GF/F 0.7 µm) and transferred into 50 ml plastic centrifuge tubes. Nutrient samples were frozen and later analyzed for NO_3^-, NO_2^-, NH_4^+, and PO_4^{3-} on a Seal Analytical AA3 HR Nutrient Analyzer at the University of Hawai'i SOEST Laboratory for Analytical Biochemistry (Table S2 in Supplement 1). GF/F filters were folded in half, wrapped in aluminum foil, and frozen for chlorophyll *a* analysis using a Turner Designs 10AU Benchtop Fluorometer (Table S2). The ratio of dissolved inorganic nitrogen to dissolved inorganic phosphate (DIN:DIP) was used as a proxy for resource quality available to filter feeders (Hauss et al. 2012), assuming that elemental composition of planktonic prey will be influenced by elemental composition of the water column, and was calculated from $([NO_3^-] + [NO_2^-] + [NH_4^+]):[PO_4^{3-}])$.

pH and total alkalinity (TA). Mean and variance in pH at each block was calculated from water samples along the transect. Water samples for pH were immediately transferred into 25 ml borosilicate glass vials, brought to a constant temperature of 25°C in a water bath, and immediately analyzed using an m-cresol dye addition spectrophotometric technique and calibrated against a Tris buffer of known pH from Andrew Dickson's Laboratory at Scripps Institution of Oceanography (Table S2). TA was fixed with 100 µl of $HgCl_2$ and analyzed using open cell potentiometric titrations on a Mettler T50 autotitrator and calibrated against a Certified Reference Material following Dickson et al. (2007) protocols. *In situ* pH and all other carbonate parameters (see Table S1) were estimated using CO2SYS (van Heuven et al. 2011) with the following parameters: pH, TA, temperature, and salinity. The K1K2 dissociation constants were from Mehrbach (1973) (refit by Dickson & Millero 1987) and HSO_4^- dissociation constants were taken from Uppström (1974) and Dickson (1990). Accuracy for TA and pH was better than 0.8 and 0.04%, respectively, and the precision was 3.55 µEq and 0.004 pH units.

Temperature. Temperature sensors (YSI 6560) were thermistors with manufacturer-reported accuracy of ±0.15°C and resolution of 0.01°C (YSI Incorporated). Average differences in temperature along the transect were small and measured as a relative anomaly from the permanent station: $(x_{mobile} - x_{permanent})/x_{permanent}$. To measure relative variability in temperature across the transect, we calculated the covariance in temperature between the mobile and permanent sensor arrays over a 2 wk period and compared this covariance across the transect.

Depth and distance from shore. Depth is the average depth measured at each block over the 2 wk deployment of the mobile station. Distance from shore is the along-transect distance (Fig. 1e).

Model selection. Our goal was to compare pH with other known drivers and correlates of the accretion-erosion balance. In a model selection framework, we used Aikake Information Criterion (AIC) values to rank candidate models, accounting for both fit and complexity. Carefully constructed model selection avoids problems associated with multiple hypothesis testing that are common in stepwise regression, such as arbitrary α levels and uninterpretable functional relationships (Johnson & Omland 2004, Anderson 2008). Here, we used the corrected AIC (AIC_c), which is recommended for sample sizes <30 (Anderson 2008). While the model with the smallest AIC_c value ($\Delta AIC_c = 0$) is the 'best' of the models considered, models with an ΔAIC_c value of <4 have some empirical support. Models with a ΔAIC_c value greater than 10 to 12 are less plausible (Anderson 2008).

Good inference from multivariate analyses is confounded by collinearity among environmental variables. Many of the environmental variables were collinear along the transect (Fig. S5 in Supplement 1); thus, we removed collinearity by using the residuals of a regression of each environmental variable against depth and distance from shore. Correlation coefficients for raw environmental data and the residual environmental data are shown in Fig. S5. Model selection with all raw data is presented in Table S3 in Supplement 1.

We compared models for 5 specific hypotheses about the accretion-erosion balance (carbonate chemistry, resource availability, temperature, depth, and distance from shore) to test which of these drivers had the strongest relationship to net accretion-erosion (Table 1). Because recent studies have demonstrated that pH variability correlates with calcification rates on coral reefs (Price et al. 2012), we measured spatial variation in both the mean and temporal variability of each environmental parameter. We used pH to test how carbonate chemistry influenced net accretion-erosion rates. Carbonate chemistry parameters are inherently correlated, and pH had the strongest relationship of the carbonate chemistry parameters (Table S4 in Supplement 1). The pH model includes both the mean and variance of the discrete pH samples from each block. The resource availability model includes the means and variances of DIN:DIP ratios (a proxy for resource quality) and chlorophyll *a* (a measure of resource quantity) from the discrete water samples. The temperature model included the mean relative temperature anomaly of each block from the permanent station and temperature covariance between the mobile and permanent stations. The final 2 models were individual models for depth and distance from shore. These linear models were compared to a full model that includes the means and variances of every parameter stated above (Table 1). Environmental data that did not meet the assumptions of normality were log-transformed and net erosion data were square-root transformed.

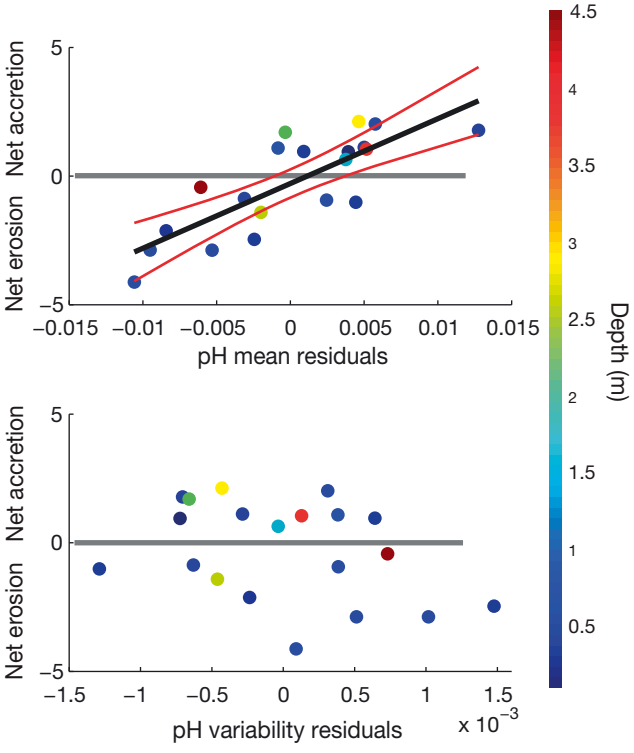

Fig. 3. Change in volume (% net accretion or erosion) of experimental coral blocks (n = 20) versus (a) mean pH residuals ($y = 251.81x - 0.29$, $R^2 = 0.64$) and (b) pH variance residuals ($y = -960.66x - 0.27$, $R^2 = 0.12$). Black and red lines in (a) show the best fit model and 95% confidence intervals respectively. Both pH mean and variance were regressed against depth and distance from shore, and the residuals were used in the analysis as shown in this figure. Percent change in volume for each block was square-root transformed to meet model assumptions

RESULTS

There were considerable differences in both the mean and variance of pH and nutrients across the 32 m transect. Mean pH increased from 7.84 to 7.91 and the coefficient of variation decreased from 0.013 to 0.0032 from onshore to offshore (Fig. 1b, Tables S1 & S5 in Supplement 1). Mean DIN:DIP decreased from 87.5 to 42.4 and the coefficient of variation increased from 0.36 to 0.59 (Fig. 1d, Table S5) from onshore to offshore. Chlorophyll *a* and temperature remained relatively constant across the spatial gradient (Fig. 1a,c, Table S5).

We compared models of pH, resource availability, temperature, depth, and distance from shore as drivers of net accretion and erosion (Table 1, Figs. S3 & S4). The pH model best explained patterns in the accretion-erosion balance along the transect in both the residual and raw data models (Tables 1 & S3, Fig. 3). Accretion was higher on the deeper reef slope, where pH is higher and less variable (Fig. 1, Figs. S6 & S7 in Supplement 1). Removing the effects of depth and distance from shore, pH was an even better predictor of the accretion-erosion balance (Figs. 3 & S3), particularly on the reef flat, and it explains 64% of the variation in net accretion-erosion over a one year deployment (Table 1). The second best model, the depth model ($\Delta AIC_c = 16.30$), explained only 6% of the variance (Table 1, Fig. S7), followed by the distance model which explained only 2% of the variance. While the resource availability model described 18% of the variance in the data, it also had a larger number of parameters (6, including mean and variance for both DIN:DIP and chlorophyll *a*) and, therefore, ranked sixth in model parsimony.

We also tested whether the mean or variance in pH was a better predictor of net accretion-erosion. Mean pH was the best model, explaining 64% of the vari-

ance (Table 1) and had a strong negative relationship with net accretion-erosion (Fig. 3). pH was also a better predictor of net accretion-erosion than TA, pCO_2, and DIC, but these highly collinear carbonate chemistry parameters did have some empirical support and explained between 42 and 58% of the variance in net accretion-erosion (Table S4).

DISCUSSION

Spatial and temporal variation in pH across the transect

Across the transect, pH had a range of 0.33 pH units at the most variable site and 0.08 pH units at the least variable site over the year (Table S1). The organisms at these sites experience a natural variation in pH that is within the range that mean pH is predicted to decrease for the 21st century (Bopp et al. 2013). Indeed, this pH range is not unique to our transect, but is typical of other shallow coral reef sites in the Pacific. For example, pH at the CRIMP2 buoy, a slightly deeper (~3 m) nearby reef site located in central Kāneʻohe Bay, ranged from 7.90 to 8.13 over a 2.5 yr study (Drupp et al. 2013). On a Palmyra reef terrace, pH ranged from 7.85 to 8.10 (Hofmann et al. 2011) and pH spanned 0.39 units in a study examining the spatial variability in microhabitats on the Great Barrier Reef (Gagliano et al. 2010). Additionally, Gagliano et al. (2010) found a similar inshore-offshore pattern: mean pH was lower and more variable inshore compared to offshore sites, though their study was conducted over a much larger spatial scale. The patterns in the means and variances here and in other studies arise from both physical and biological processes including: tidal mixing with offshore waters, photosynthesis/respiration (P/R) cycles, and reef metabolism (Hurd et al. 2011, Kleypas et al. 2011), upwelling events (Leichter et al. 2003, Manzello et al. 2008), and porewater advection from permeable sediments (Santos et al. 2011). We saw a very strong correlation between pH variance and distance from shore (Fig. S6), suggesting that tidal mixing was an important contributor to the spatial variation in pH, although we did not specifically test this hypothesis. Using the residual values that remove the effect of distance and depth from pH eliminates the impact of this large-scale mixing, leaving the effect of small-scale processes (such as local P/R and turbulent mixing) on pH. The raw pH data model explained 48% of the variance in net accretion-erosion (Table S3), but the residual model was an even better fit (Table 1), suggesting that small-scale physicochemical differences in microhabitats may strongly influence the patterns of accretion and erosion on coral reefs. The results of this study suggest that differences in microhabitat variability may be more important to the accretion-erosion balance than larger-scale processes. A better characterization of microhabitat variability (see Guadayol et al. 2014) and how this microhabitat variation impacts reefs will help predict reef responses to climate change in the context of natural variability.

Implications for the accretion-erosion balance of coral reefs

Our results show that differences in the seawater chemistry on the scale of meters can have a substantial influence on the accretion-erosion balance. The majority of the blocks with mean pH <7.88 were net eroding (Fig. S3); this pH value is likely to become more prevalent with the predicted 0.3 to 0.4 pH unit reduction in oceanic waters (Orr et al. 2005, Bopp et al. 2013). Previous studies on coral reefs have shown shifts from net accretion to erosion after major disturbances, such as El Niño-Southern Oscillation (ENSO) events or hurricanes (Perry et al. 2008). Our data indicate that pH is a significant driver of net reef erosion and that, as mean pH decreases, erosion rates will increase. The pH model ranked higher than the distance, depth, and resource availability models; prior studies where depth, distance, and resource availability were stronger predictors of bioerosion were performed on much larger spatial scales and covered a greater range of values (e.g. Perry 1998, Holmes et al. 2000, Tribollet et al. 2002, Le Grand & Fabricius 2011, Schmidt & Richter 2013). For instance, a prior study showing a strong response of bioerosion to resource availability had mean chlorophyll *a* values ranging from 0.25 to 1.24 µg l^{-1} across their comparison sites (Holmes et al. 2000), compared to a range of only 0.14 to 0.31 µg l^{-1} in this study (Fig. 1). Results from the current study are in agreement with recent laboratory (Tribollet et al. 2009, Wisshak et al. 2012, 2013, Fang et al. 2013, Reyes-Nivia et al. 2013) and field experiments (Manzello et al. 2008, Fabricius et al. 2011, Crook et al. 2013) suggesting that erosion rates will increase with ocean acidification. However, this is the first study to directly test the relationship between the accretion-erosion balance and pH using a natural pH gradient, and to compare this relationship to other known drivers and correlates of reef accretion and erosion.

The bioeroder community is diverse and has a number of mechanisms for boring, including chemical dissolution and mechanical erosion. Individual species respond differently to environmental parameters and, thus, influence the accretion-erosion balance through changes in individual bioerosion rates and in community composition. For example, previous studies have found that boring sponges and bivalves respond positively to eutrophication, while the response of polychaetes is more variable (Le Grand & Fabricius 2011). Filter feeding sponges and bivalves are positively correlated with eutrophic sites in the Bahamas (Rose & Risk 1985), Barbados (Holmes et al. 2000), the Red Sea (Kleemann 2001), the Great Barrier Reef (Osorno et al. 2005, Tribollet & Golubic 2005) and the eastern Pacific (Fonseca et al. 2006); bivalve abundances are also correlated with high water velocity (Cantera et al. 2003, Londono-Cruz et al. 2003). In contrast, deposit feeding polychaetes in the Great Barrier Reef are more abundant at eutrophic sites (Osorno et al. 2005), while suspension feeding polychaetes are more abundant in oligotrophic sites (Le Bris et al. 1998). In addition, there are strong successional dynamics in these communities, and patterns of succession are location specific. In the Great Barrier Reef, microborers and polychaetes are the initial colonizers; these are followed by sipunculans, bivalves, and then sponges (Hutchings 1986); it may take up to 3 yr for sponges to fully colonize dead substrate (Tribollet & Golubic 2005). In the Caribbean, the suggested successional pattern of bioeroders is algae, fungi, clionid sponges, polychaetes, bivalves, barnacles, and then sipunculans (Risk & MacGeachy 1978). In Hawai'i, an 18 mo study in Kāne'ohe Bay found no obvious successional patterns (White 1980), but likely captured only the initial successional stages. Our study highlights the influence of pH on the accretion-erosion balance after 1 yr, i.e. during the early-successional stage of this community, and future studies should include multi-year comparisons to test if this pattern holds. In a previous Kāne'ohe Bay study that used similar blocks, the most abundant organisms after a 1 yr deployment were polychaetes (Spionidae were the most abundant and largest polychaete borers) and sipunculans (White 1980). These were the most common taxa in our study as well. Parrotfish erosion was also evident on our blocks. Common secondary calcifiers in our community were crustose coralline algae (*Hydrolithon* spp.), barnacles, and the oyster *Crassostrea gigas*.

Our results highlight the value of using of µCT as a tool to calculate accretion and erosion rates on coral reefs. µCT provides a more sensitive measure of net accretion-erosion in the field than previously published methods (e.g. Edinger & Risk 1996, Tribollet et al. 2009, Perry et al. 2012), and it is directly comparable across studies. Prior studies have used single CT scans to calculate skeletal density (Bosscher 1993), skeletal porosity (Roche et al. 2010), and linear extension (Crook et al. 2013); here, we used µCT in a novel way by comparing before and after images to calculate the precise volume of $CaCO_3$ removed or accreted. As reef erosion and coral growth are often decoupled on coral reefs (Edinger et al. 2000), quantification of net erosion must complement measures of coral growth for a more complete picture of coral reef health.

Although chemical dissolution will accelerate in future decades as tropical coral reefs shift to less saturated aragonite conditions (van Woesik et al. 2013), bioerosion is currently the main driver of reef loss (Andersson & Gledhill 2013). The mechanisms by which ocean acidification may enhance bioerosion rates include: (1) lower coral skeletal densities (Hoegh-Guldberg et al. 2007, Cooper et al. 2008), making it easier for bioeroders to penetrate the coral skeleton (Edinger & Risk 1996, Dumont et al. 2013), though this point is debated in the literature (Highsmith 1981, Schönberg 2002, Hernández-Ballesteros et al. 2013); (2) increased growth rates of photosynthesizing bioeroders (Tribollet et al. 2009); (3) declines in crustose coralline algae (Jokiel et al. 2008), which can inhibit settlement and growth of micro- and macroborers (Tribollet & Payri 2001); and (4) increased susceptibility of calcifiers to grazers (Johnson & Carpenter 2012). In addition, many boring organisms excrete acidic compounds, raising the possibility that a reduction in ocean pH could make it less metabolically costly to lower pH at the site of erosion.

The combination of slower coral growth (Hoegh-Guldberg et al. 2007, Kroeker et al. 2010, Pandolfi et al. 2011) and higher erosion rates with ocean acidification could act synergistically to hinder reef growth. In the Caribbean, erosion rates are highest in areas where coral cover is low (Perry et al. 2013), indicating that the same drivers that negatively impact corals may also promote erosion. Further, given the strong relationship between bioerosion and local anthropogenic impacts like sedimentation and nutrient runoff (Edinger et al. 2000, Le Grand & Fabricius 2011), the combined effect of these local impacts with decreases in pH in the global oceans could be devastating to reefs worldwide. This study portrays how coral reef ecosystems may change under pre-

dicted increases in ocean acidity: an existing community of reef secondary calcifiers and bioeroders showed a shift from net accretion to net erosion along a naturally occurring, within-reef gradient of high to low pH.

Acknowledgements. We are grateful to C.J. Bradley, J. Chen, R. Coleman, A. Copeland, K. DiPerna, M. Donovan, N. Griffith, K. Hurley, M. Iacchei, I. Iglesias, M. Siple, E.M. Sogin, M. Sudek, J. Sziklay, M. Walton, and the Point Lab for help with data collection. We thank M. Riccio and F. von Stein from the Cornell University µCT Facility for Imaging and Preclinical Research, R. Briggs from UH SOEST Laboratory for Analytical Biochemistry, and the UH lapidary facility. Funding for this project came from NOAA Office of National Marine Sanctuaries-HIMB partnership (MOA #2009-039/7932), National Science Foundation EPSCoR Hawai'i, NOAA Dr. Nancy Foster Scholarship to N.J.S., Sigma-Xi GIAR to N.J.S., and by Hawai'i Sea Grants #1889 to F.I.M.T and #1847 to M.J.D. and F.I.M.T. This paper is funded in part by a grant/cooperative agreement from the National Oceanic and Atmospheric Administration, Project No. R/IR-18, which is sponsored by the University of Hawai'i Sea Grant College Program, School of Ocean and Earth Science and Technology, under Institutional Grant No. NA09OAR4170060 Office of Sea Grant, Department of Commerce. The views expressed herein are those of the author(s) and do not necessarily reflect the views of NOAA or any of its subagencies. Comments from H. Putnam, C. Jury, E. Wolkovich, and 3 anonymous reviewers improved this manuscript. This is HIMB contribution #1597, SOEST #9188, and SeaGrant #UNIHI-SEAGRANT-JC-13-13.

LITERATURE CITED

Anderson DR (2008) Model based inference in the life sciences: a primer on evidence. Springer

Andersson AJ, Gledhill D (2013) Ocean acidification and coral reefs: effects on breakdown, dissolution, and net ecosystem calcification. Annu Rev Mar Sci 5:321–348

Becker L, Reaka-Kudla M (1996) The use of tomography in assessing bioerosion in corals. In: Proc 8th Int Coral Reef Symp, Panama 2:1819–1824

Beuck L, Vertino A, Stepina E, Karolczak M, Pfannkuche O (2007) Skeletal response of *Lophelia pertusa* (Scleractinia) to bioeroding sponge infestation visualised with micro-computed tomography. Facies 53:157–176

Bopp L, Resplandy L, Orr JC, Doney SC and others (2013) Multiple stressors of ocean ecosystems in the 21st century: projections with CMIP5 models. Biogeosciences 10: 6225–6245

Bosscher H (1993) Computerized-tomography and skeletal density of coral skeletons. Coral Reefs 12:97–103

Caldeira K, Wickett ME (2003) Oceanography: anthropogenic carbon and ocean pH. Nature 425:365–365

Cantera JRK, Orozco C, Londono-Cruz E, Toro-Farmer G (2003) Abundance and distribution patterns of infaunal associates and macroborers of the branched coral (*Pocillopora damicornis*) in Gorgona Island (eastern tropical Pacific). Bull Mar Sci 72:207–219

Cooper TF, De'Ath G, Fabricius KE, Lough JM (2008) Declining coral calcification in massive *Porites* in two nearshore regions of the northern Great Barrier Reef. Glob Change Biol 14:529–538

Crook ED, Cohen AL, Rebolledo-Vieyra M, Hernandez L, Paytan A (2013) Reduced calcification and lack of acclimatization by coral colonies growing in areas of persistent natural acidification. Proc Natl Acad Sci USA 110: 11044–11049

Davidson TM, de Rivera CE, Carlton JT (2013) Small increases in temperature exacerbate the erosive effects of a non-native burrowing crustacean. J Exp Mar Biol Ecol 446:115–121

Dickson AG (1990) Standard potential of the reaction: AgCl(s) + ½H_2(g) = Ag(s) + HCl(aq), and and the standard acidity constant of the ion HSO_4^- in synthetic sea water from 273.15 to 318.15 K. J Chem Thermodyn 22: 113–127

Dickson A, Millero F (1987) A comparison of the equilibrium constants for the dissociation of carbonic acid in seawater media. Deep-Sea Res A, Oceanogr Res Pap 34: 1733–1743

Dickson A, Sabine C, Christian JR (2007) Guide to best practices for ocean CO_2 measurements. PICES Special Publication 3

Drupp P, De Carlo EH, Mackenzie FT, Bienfang P, Sabine CL (2011) Nutrient inputs, phytoplankton response, and CO_2 variations in a semi-enclosed subtropical embayment, Kaneohe Bay, Hawaii. Aquat Geochem 17: 473–498

Drupp PS, De Carlo EH, Mackenzie FT, Sabine CL, Feely RA, Shamberger KE (2013) Comparison of CO_2 dynamics and air–sea gas exchange in differing tropical reef environments. Aquat Geochem 19:371–397

Duarte CM, Hendriks IE, Moore TS, Olsen YS and others (2013) Is ocean acidification an open-ocean syndrome? Understanding anthropogenic impacts on seawater pH. Estuaries Coasts 36:1–16

Dumont CP, Lau DC, Astudillo JC, Fong KF, Chak ST, Qiu JW (2013) Coral bioerosion by the sea urchin *Diadema setosum* in Hong Kong: susceptibility of different coral species. J Exp Mar Biol Ecol 441:71–79

Edinger EN, Risk MJ (1996) Sponge borehole size as a relative measure of bioerosion and paleoproductivity. Lethaia 29:275–286

Edinger EN, Limmon GV, Jompa J, Widjatmoko W, Heikoop JM, Risk MJ (2000) Normal coral growth rates on dying reefs: Are coral growth rates good indicators of reef health? Mar Pollut Bull 40:404–425

Fabricius K, Langdon C, Uthicke S, Humphrey C and others (2011) Losers and winners in coral reefs acclimatized to elevated carbon dioxide concentrations. Nat Clim Change 1:165–169

Fang JK, Mello-Athayde MA, Schönberg CH, Kline DI, Hoegh-Guldberg O, Dove S (2013) Sponge biomass and bioerosion rates increase under ocean warming and acidification. Glob Change Biol 19:3581–3591

Feely RA, Sabine CL, Lee K, Berelson W, Kleypas J, Fabry VJ, Millero FJ (2004) Impact of anthropogenic CO_2 on the $CaCO_3$ system in the oceans. Science 305:362–366

Fonseca AC, Dean HK, Cortes J (2006) Non-colonial coral macro-borers as indicators of coral reef status in the south pacific of Costa Rica. Rev Biol Trop 54:101–115

Gagliano M, McCormick MI, Moore JA, Depczynski M (2010) The basics of acidification: baseline variability of pH on Australian coral reefs. Mar Biol 157:1849–1856

Grigg RW (1982) Darwin point: a threshold for atoll formation. Coral Reefs 1:29–34

Guadayol Ò, Silbiger NJ, Donahue MJ, Thomas FI (2014) Patterns in temporal variability of temperature, oxygen and pH along an environmental gradient in a coral reef. PLoS ONE 9:e85213

Guinotte JM, Fabry VJ (2008) Ocean acidification and its potential effects on marine ecosystems. Ann N Y Acad Sci 1134:320–342

Hauss H, Franz J, Sommer U (2012) Changes in N:P stoichiometry influence taxonomic composition and nutritional quality of phytoplankton in the Peruvian upwelling. J Sea Res 73:74–85

Hernández-Ballesteros LM, Elizalde-Rendón EM, Carballo JL, Carricart-Ganivet JP (2013) Sponge bioerosion on reef-building corals: dependent on the environment or on skeletal density? J Exp Mar Biol Ecol 441:23–27

Highsmith RC (1981) Coral bioerosion: damage relative to skeletal density. Am Nat 117:193–198

Hoegh-Guldberg O, Mumby PJ, Hooten AJ, Steneck RS and others (2007) Coral reefs under rapid climate change and ocean acidification. Science 318:1737–1742

Hofmann GE, Smith JE, Johnson KS, Send U and others (2011) High-frequency dynamics of ocean pH: a multi-ecosystem comparison. PLoS ONE 6:e28983

Holmes KE (2000) Effects of eutrophication on bioeroding sponge communities with the description of new West Indian sponges, *Cliona* spp. (Porifera: Hadromerida: Clionidae). Invertebr Biol 119:125–138

Holmes KE, Edinger EN, Hariyadi, Limmon GV, Risk MJ (2000) Bioerosion of live massive corals and branching coral rubble on Indonesian coral reefs. Mar Pollut Bull 40:606–617

Hubbard DK, Miller AI, Scaturo D (1990) Production and cycling of calcium carbonate in a shelf-edge reef system (St. Croix, US Virgin Islands): application to the nature of reef systems in the fossil record. J Sediment Petrol 60: 335–360

Hurd CL, Cornwall CE, Currie K, Hepburn CD, McGraw CM, Hunter KA, Boyd PW (2011) Metabolically induced pH fluctuations by some coastal calcifiers exceed projected 22nd century ocean acidification: a mechanism for differential susceptibility? Glob Change Biol 17: 3254–3262

Hutchings PA (1986) Biological destruction of coral reefs: a review. Coral Reefs 4:239–252

Johnson MD, Carpenter RC (2012) Ocean acidification and warming decrease calcification in the crustose coralline alga *Hydrolithon onkodes* and increase susceptibility to grazing. J Exp Mar Biol Ecol 434-435:94–101

Johnson JB, Omland KS (2004) Model selection in ecology and evolution. Trends Ecol Evol 19:101–108

Jokiel PL, Rodgers KS, Kuffner IB, Andersson AJ, Cox EF, Mackenzie FT (2008) Ocean acidification and calcifying reef organisms: a mesocosm investigation. Coral Reefs 27:473–483

Kleemann K (2001) The pectinid bivalve *Pedum spondyloideum* (Gmelin 1791): amount of surface and volume occupied in host corals from the Red Sea. Mar Ecol 22: 111–133

Kleypas JA, Anthony K, Gattuso JP (2011) Coral reefs modify their seawater carbon chemistry — case study from a barrier reef (Moorea, French Polynesia). Glob Change Biol 17:3667–3678

Kroeker KJ, Kordas RL, Crim RN, Singh GG (2010) Meta-analysis reveals negative yet variable effects of ocean acidification on marine organisms. Ecol Lett 13: 1419–1434

Le Bris S, Le Campion-Alsumard T, Romano JC (1998) Characteristics of epilithic and endolithic algal turf exposed to different levels of bioerosion in French Polynesian coral reefs. Oceanol Acta 21:695–708

Le Grand HM, Fabricius KE (2011) Relationship of internal macrobioeroder densities in living massive *Porites* to turbidity and chlorophyll on the Australian Great Barrier Reef. Coral Reefs 30:97–107

Leichter JJ, Stewart HL, Miller SL (2003) Episodic nutrient transport to Florida coral reefs. Limnol Oceanogr 48: 1394–1407

Londono-Cruz E, Cantera JR, Toro-Farmer G, Orozco C (2003) Internal bioerosion by macroborers in *Pocillopora* spp. in the tropical eastern Pacific. Mar Ecol Prog Ser 265:289–295

Lowe RJ, Falter JL, Monismith SG, Atkinson MJ (2009a) A numerical study of circulation in a coastal reef-lagoon system. J Geophys Res 114:C06022

Lowe RJ, Falter JL, Monismith SG, Atkinson MJ (2009b) Wave-driven circulation of a coastal reef-lagoon system. J Phys Oceanogr 39:873–893

Manzello DP, Kleypas JA, Budd DA, Eakin CM, Glynn PW, Langdon C (2008) Poorly cemented coral reefs of the eastern tropical Pacific: possible insights into reef development in a high-CO_2 world. Proc Natl Acad Sci USA 105:10450–10455

Massaro RF, De Carlo EH, Drupp PS, Mackenzie FT and others (2012) Multiple factors driving variability of CO_2 exchange between the ocean and atmosphere in a tropical coral reef environment. Aquat Geochem 18:357–386

Mehrbach C (1973) Measurement of the apparent dissociation constants of carbonic acid in seawater at atmospheric pressure. Limnol Oceanogr 18:897–907

Moran DP, Reaka ML (1988) Bioerosion and availability of shelter for benthic reef organisms. Mar Ecol Prog Ser 44: 249–263

Neumann AC (1966) Observations on coastal erosion in Bermuda and measurements of boring rate of sponge *Cliona lampa*. Limnol Oceanogr 11:92–108

Orr JC, Fabry VJ, Aumont O, Bopp L and others (2005) Anthropogenic ocean acidification over the twenty-first century and its impact on calcifying organisms. Nature 437:681–686

Osorno A, Peyrot-Clausade M, Hutchings PA (2005) Patterns and rates of erosion in dead *Porites* across the Great Barrier Reef (Australia) after 2 years and 4 years of exposure. Coral Reefs 24:292–303

Pandolfi JM, Connolly SR, Marshall DJ, Cohen AL (2011) Projecting coral reef futures under global warming and ocean acidification. Science 333:418–422

Perry CT (1998) Macroborers within coral framework at Discovery Bay, north Jamaica: species distribution and abundance, and effects on coral preservation. Coral Reefs 17:277–287

Perry CT, Spencer T, Kench PS (2008) Carbonate budgets and reef production states: a geomorphic perspective on the ecological phase-shift concept. Coral Reefs 27: 853–866

Perry CT, Edinger E, Kench P, Murphy G, Smithers S, Steneck R, Mumby P (2012) Estimating rates of biologically driven coral reef framework production and erosion: a new census-based carbonate budget methodology and applications to the reefs of Bonaire. Coral Reefs 31: 853–868

Perry CT, Murphy G, Kench P, Smithers S, Edinger E, Steneck R, Mumby P (2013) Caribbean-wide decline in carbonate production threatens coral reef growth. Nat Commun 4:1402

Price NN, Martz T, Brainard R, Smith J (2012) Diel variability in seawater pH relates to calcification and benthic community structure on coral reefs. PLoS ONE 7:e43843

Reyes-Nivia C, Diaz-Pulido G, Kline D, Guldberg OH, Dove S (2013) Ocean acidification and warming scenarios increase microbioerosion of coral skeletons. Glob Change Biol 19:1919–1929

Ries JB, Cohen AL, McCorkle DC (2009) Marine calcifiers exhibit mixed responses to CO_2-induced ocean acidification. Geology 37:1131–1134

Risk M, MacGeachy J (1978) Aspects of bioerosion of modern caribbean reefs. Rev Biol Trop 26:85–105

Risk MJ, Sammarco PW, Edinger EN (1995) Bioerosion in *Acropora* across the continental shelf of the Great Barrier Reef. Coral Reefs 14:79–86

Roche RC, Abel RA, Johnson KG, Perry CT (2010) Quantification of porosity in *Acropora pulchra* (Brook 1891) using X-ray micro-computed tomography techniques. J Exp Mar Biol Ecol 396:1–9

Roche R, Abel R, Johnson K, Perry C (2011) Spatial variation in porosity and skeletal element characteristics in apical tips of the branching coral *Acropora pulchra* (Brook 1891). Coral Reefs 30:195–201

Rose CS, Risk MJ (1985) Increase in *Cliona delitrix* infestation of *Montastrea cavernosa* heads on an organically polluted portion of the Grand Cayman fringing reef. Mar Ecol 6:345–363

Sabine CL, Feely RA, Gruber N, Key RM and others (2004) The oceanic sink for anthropogenic CO_2. Science 305: 367–371

Santos IR, Glud RN, Maher D, Erler D, Eyre BD (2011) Diel coral reef acidification driven by porewater advection in permeable carbonate sands, Heron Island, Great Barrier Reef. Geophys Res Lett 38:L03604, doi:10.1029/2010GL-046053

Schmidt GM, Richter C (2013) Coral growth and bioerosion of *Porites lutea* in response to large amplitude internal waves. PLoS ONE 8:e73236

Schönberg CH (2002) Substrate effects on the bioeroding demosponge *Cliona orientalis*. 1. Bioerosion rates. Mar Ecol (Berl) 23:313–326

Schönberg CH, Shields G (2008) Micro-computed tomography for studies on *Entobia*: transparent substrate versus modern technology. In: Wisshak M, Tapanila L (eds) Current developments in bioerosion. Springer, Berlin, p 147–164

Scott PJB, Risk MJ (1988) The effect of *Lithophaga* (Bivalvia, Mytilidae) boreholes on the strength of the coral *Porites lobata.* Coral Reefs 7:145–151

Silverman J, Lazar B, Cao L, Caldeira K, Erez J (2009) Coral reefs may start dissolving when atmospheric CO_2 doubles. Geophys Res Lett 36:L05606, doi:10.1029/2008GL-036282

Smith SV, Kimmerer WJ, Laws EA, Brock RE, Walsh TW (1981) Kaneohe Bay sewage diversion experiment: perspectives on ecosystem responses to nutritional perturbation. Pac Sci 35:279–402

Smith JE, Price NN, Nelson CE, Haas AF (2013) Coupled changes in oxygen concentration and pH caused by metabolism of benthic coral reef organisms. Mar Biol 160:2437–2447

Tribollet A (2008) The boring microflora in modern coral reef ecosystems: a review of its roles. Current developments in bioerosion. Springer, Berlin, p 67–94

Tribollet A, Golubic S (2005) Cross-shelf differences in the pattern and pace of bioerosion of experimental carbonate substrates exposed for 3 years on the northern Great Barrier Reef, Australia. Coral Reefs 24:422–434

Tribollet A, Payri C (2001) Bioerosion of the coralline alga *Hydrolithon onkodes* by microborers in the coral reefs of Moorea, French Polynesia. Oceanol Acta 24:329–342

Tribollet A, Decherf G, Hutchings PA, Peyrot-Clausade M (2002) Large-scale spatial variability in bioerosion of experimental coral substrates on the Great Barrier Reef (Australia): importance of microborers. Coral Reefs 21: 424–432

Tribollet A, Godinot C, Atkinson M, Langdon C (2009) Effects of elevated pCO_2 on dissolution of coral carbonates by microbial euendoliths. Global Biogeochem Cycles 23:GB3008, doi:10.1029/2008GB003286

Uppström LR (1974) The boron/chlorinity ratio of deep-sea water from the Pacific Ocean. Deep-Sea Res 21: 161–162

van Heuven S, Pierrot D, Rae J, Lewis E, Wallace D (2011) MATLAB program developed for CO_2 system calculations. ORNL/CDIAC-105b. Carbon Dioxide Information Analysis Center, Oak Ridge National Laboratory, US Department of Energy, Oak Ridge, TN

van Woesik R, van Woesik K, van Woesik L, van Woesik S (2013) Effects of ocean acidification on the dissolution rates of reef-coral skeletons. Peer J 1:e208

White J (1980) Distribution, recruitment and development of the borer community in dead coral on shallow Hawaiian reefs. PhD thesis, University of Hawaii at Manoa

Wisshak M, Schönberg CH, Form A, Freiwald A (2012) Ocean acidification accelerates reef bioerosion. PLoS ONE 7:e45124

Wisshak M, Schönberg C, Form AU, Freiwald A (2013) Effects of ocean acidification and global warming on reef bioerosion — lessons from a clionaid sponge. Aquat Biol 19:111–127

Yates KK, Dufore C, Smiley N, Jackson C, Halley RB (2007) Diurnal variation of oxygen and carbonate system parameters in Tampa Bay and Florida Bay. Mar Chem 104:110–124

Editorial responsibility: Brian Helmuth, Nahant, Massachusetts, USA

Submitted: January 14, 2014; Accepted: August 17, 2014
Proofs received from author(s): October 27, 2014